Ceramics International 44 (2018) 15588–15595

Contents lists available at ScienceDirect

Ceramics International

journal homepage: www.elsevier.com/locate/ceramint

Effects of strontium/lanthanum co-doping on the dielectric properties of $CaCu_3Ti_4O_{12}$ prepared by reactive sintering

Rodrigo Espinoza-González[a,*], Samuel Hevia[b,c], Álvaro Adrian[b]

[a] LabMAM, Departamento de Ingeniería Química Biotecnología y Materiales, FCFM, Universidad de Chile, Santiago, Chile
[b] Instituto de Física, Pontificia Universidad Católica de Chile, Casilla 306, Santiago 6904411, Chile
[c] Centro de Investigación en Nanotecnología y Materiales Avanzados, Pontificia Universidad Católica de Chile, Casilla 306, Santiago 6904411, Chile

ARTICLE INFO

Keywords:
CCTO
Co-doping
Dielectric
Modulus spectroscopy
Reactive sintering

ABSTRACT

The extremely high dielectric constant of the cubic perovskite $CaCu_3Ti_4O_{12}$ (CCTO) has attracted increasing attention for a variety of capacitive elements in microelectronic device applications. In this research, the influence of Sr and La replacing Ca and Cu, respectively, to simultaneously controlling the intrinsic properties of grain boundaries in a co-doped CCTO ceramic has been investigated. The preparation was done using high purity compounds milled and mixed by mechano-synthesis and further consolidated by reactive sintering without calcination. Characterization by XRD confirmed the formation of single-phase CCTO ceramic and a residual amount $CaTiO_3$. The microstructure and composition analyzed by SEM/EDX showed a smaller grain size for the co-doped CCTO. Impedance measurements indicated the smallest dielectric loss for the co-doped ceramics compare to pure and single-doped CCTO, while reaching a higher dielectric permittivity than single-doped ceramics. The CCTO-SrLa sample also showed high thermal stability of the dielectric permittivity between 100 and 470 K, and the lowest loss between 200 and 300 K. This behavior was attributed to the lower bulk resistance exhibited by the co-doped sample.

1. Introduction

Ceramics with colossal dielectric constant (CDC) have been intensively studied for their potential use as supercapacitors and in microelectronic applications [1–3]. One of the interesting candidates is the ceramic compound, calcium copper titanate, $CaCu_3Ti_4O_{12}$ (CCTO) that has attracted the attention of many researchers due to its CDC. CCTO is a well-known ceramic material that has a dielectric constant in the order of 10^4 and a dielectric loss of around 0.1 at 1 kHz; and a nonlinear current voltage characteristic up to 10^6 Hz over a broad temperature range (from 100 to 600 K) [4]. CCTO is a body-centered cubic oxide with four $ATiO_3$ units per primitive cell, where Ca^{2+} and Cu^{2+} ions reside in the A-sites while Ti cations occupy the B-sites. The size difference between the A-site causes a substantial tilting in the TiO_6 octahedra, leading to a body centered cubic super cell [5]. Several researchers have tried to explain the origin of giant dielectric constant of this material by different models. Sinclair et al. [6] demonstrated that CCTO ceramic consists of semiconducting grains with insulating grain boundaries. Thus, the higher dielectric constant would come from an internal-barrier-layer-capacitance (IBLC) effect. Ramirez et al. [7] proposed that the collective ordering of local dipole moments is the source of unusual high dielectric response and explained it by a highly polarizable relaxational excitations model. On the other hand, Lunkenheimer et al. [8] considered the contact-electrode depletion effect as an explanation for the high value of the dielectric constant.

In order to promote the practical applications of CCTO, many studies have been done to reduce the dielectric loss in this material. Much of this work is based upon cation substitution at A- or B-sites to improve the dielectric properties and extend the understanding on the origin of the CDC [9–18]. Different authors [11–13] have doped CCTO by adding La^{3+} in Ca position and showed a reduction of the real part of the dielectric constant (ε_r) and also of the dielectric loss ($\tan\delta$) compared to pure CCTO. Similarly, Xue et al. [14] doped CCTO by using Sr in Ca position, which decreases the dielectric constant but with a minor reduction of the dielectric loss. Analogous results were published by Vangchangyia et al. [16] and Yang et al. [15].

Recently, co-doping has been established as a new strategy to suppress the grain growth and grain boundary resistivity [19–24] with a significant impact on the dielectric properties. The strategy behind co-doping is to simultaneously suppress the grain growth and to enhance the grain boundary resistivity in order to reduce the dielectric loss [19] by doping different sites in the CCTO crystalline structure. Boonlakhorn

* Corresponding author.
E-mail address: roespino@ing.uchile.cl (R. Espinoza-González).

https://doi.org/10.1016/j.ceramint.2018.05.223
Received 5 March 2018; Received in revised form 17 May 2018; Accepted 25 May 2018
Available online 26 May 2018

et al. reported promising results by using combinations of dopants in the Ca^{2+} and Cu^{2+} sites like for example Sm/Mg [19], Y/Mg [20] and Yb/Mg [21].

Alternatively, reaction-sintering has been used to prepare CCTO obtaining a very similar dielectric behavior compared to those prepared by conventional synthesis [25,26]. Rubia et al. studied Hf-doped CCTO ceramics prepared by reaction sintering, demonstrating a higher incorporation of the dopant during reactive sintering. Espinoza et al. [26] also used reactive sintering in CCTO powders milled in a Spex mill. They obtained similar dielectric properties to CCTO prepared by conventional solid state reaction, without an intermediate calcination step meaning a reduction of the energy required for the preparation of the ceramic.

In this communication, the dielectric properties of Sr/La co-doped CCTO, prepared by reactive sintering, were investigated and compared with results obtained for un-doped and single-doped CCTO with Sr and La. The aim of this work is the reduction of the dielectric loss to promote the use of CCTO ceramic in microelectronic applications.

2. Experimental procedure

The starting materials for the synthesis of CCTO powders were $CaCO_3$ (Merck, 99.95%), CuO (Sigma-Aldrich, 99.99%), and anatase-TiO_2 (Sigma-Aldrich, 99.8%). The corresponding stoichiometric amounts of precursor powders were weighed with the respective amounts of dopants La_2O_3 (Sigma-Aldrich, 99.99%), $SrCO_3$ (Sigma-Aldrich, 99.9%) to prepare pure and doped CCTO by high-energy mechano-synthesis in a Spex Dual Mill 8000D, which operates at 875 cycles per minute. Based upon preliminary experiments, the selected dopant concentrations and cation replacement were as follows: $Ca_{0.6}Sr_{0.4}Cu_3Ti_4O_{12}$, $CaCu_{2.85}La_{0.15}Ti_4O_{12}$, $Ca_{0.6}Sr_{0.4}Cu_{2.85}La_{0.15}Ti_4O_{12}$ and, pure $CaCu_3Ti_4O_{12}$. The samples prepared for each composition were named: CCTO-Sr, CCTO-La, CCTO-SrLa and CCTO, respectively.

The powders were wet milled with ethanol as milling media during 2 h using stainless steel vials and balls, with a ball to powder ratio (BPR) of 5:1. Subsequently, reactive sintering was used to simultaneously obtain the CCTO phase and to consolidate the powders. Thus, the milled powders were compacted into discs by uniaxial pressing and sintered in air at 1050 °C for 18 h. The samples after sintering had a thickness of 1.6 mm and a diameter of 8.8 mm. Sintered pellets were characterized by X-ray diffraction (XRD) in a Bruker D8 diffractometer using CuKα radiation. The data were collected at room temperature with a step size and scan rate of 0.01° and 0.1 s, respectively. The X-ray tube was operated at 40 kV and 30 mA. Rietveld refinement of XRD patterns was performed using TOPAS software, for which pseudo-Voigt function was chosen as a profile function. In all refinements, the good of fitness (GOF) parameter was smaller than 1.8. The microstructure and composition were studied by field emission scanning electron microscopy (FESEM, FEI microscope, model Quanta 250) with an EDAX detector for energy-dispersive X-ray spectroscopy (EDX). Prior to SEM/

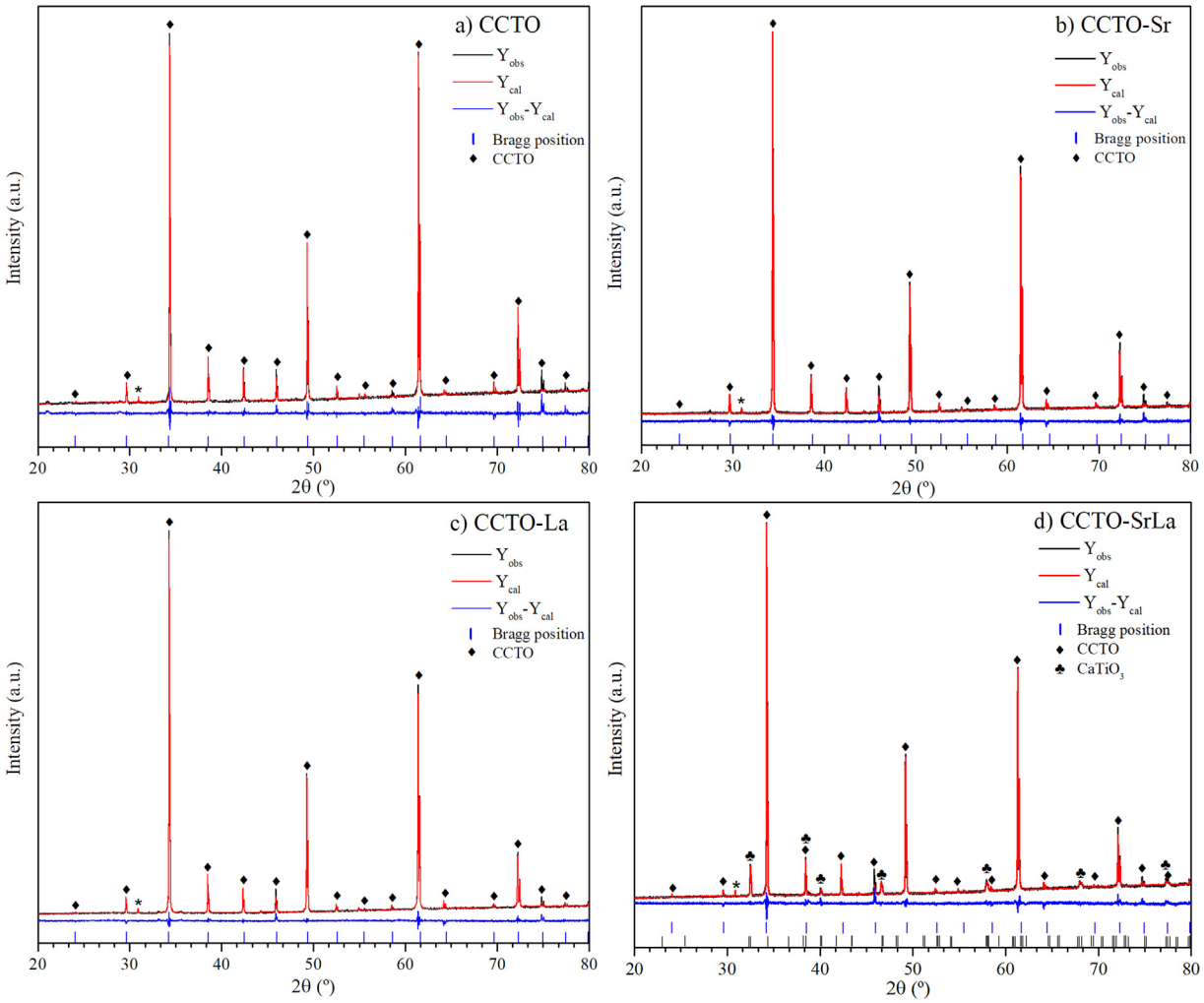

Fig. 1. Structure refinements of pure and doped CCTO samples: a) pure CCTO, b) CCTO-Sr, c) CCTO-La, and d) CCTO-SrLa. (*) Peaks corresponding to K_β reflection of CCTO (022).

Table 1
Lattice parameter (a), Rietveld refinement parameters and relative density (ρ).

Sample	a (nm)	R_{exp} (%)	R_{wp} (%)	R_p (%)	GOF	ρ (%)
CCTO	0.7397(5)	3.64	5.75	4.08	1.58	91
CCTO-Sr	0.7403(1)	3.39	6.38	4.41	1.88	93
CCTO-La	0.7397(1)	3.73	6.31	4.45	1.69	90
CCTO-SrLa	0.7405(4)	3.68	6.41	4.52	1.74	92

EDX analysis, the samples were polished and thermally etched at 1000 °C during 30 min. The grain size was obtained from the SEM micrographs by direct measurement using the software ImageJ. For impedance measurements, gold electrodes were sputtered onto both polished surfaces of sintered samples thus leading to an electrode area of 61 mm^2. Impedance measurements were performed at room temperature in the frequency range between 20 and 10 MHz with an applied voltage of 1 V, using a Keysight Impedance Analyzer E4990A. The same equipment was used to measure impedance behavior between 55 and 445 K in a closed cooling system (Janis).

3. Results and discussion

3.1. X-Ray diffraction results

Fig. 1 shows the XRD patterns of pure and doped CCTO samples. In the case of pure and single doped samples, XRD analysis confirmed the single-phase formation of the pseudo-cubic CCTO compound by comparing the obtained XRD pattern with the standard powder diffraction file database (JCPDS File No. 75-1149). The pattern of the co-doped CCTO-SrLa sample showed the presence of the same CCTO phase and the secondary formation of $CaTiO_3$ (JCPDS File No. 42-0423).

Rietveld refinement confirmed the mentioned phases for all samples and gave values for the unit cell parameter (a) for the CCTO phase (see Table 1). Pure CCTO and CCTO-La have a lattice parameter very close to the reported value of the JCPDS, while the other samples have a slightly higher value compared to the pure CCTO sample. Based upon this observation, it can be concluded, that Sr is effectively introduced into the crystalline structure while La may have formed a phase, which is not detectable by this technique. Additionally, by Rietveld refinement, it can be also shown that the sample CCTO-SrLa has a 10 wt% of $CaTiO_3$ as a secondary phase.

The relative density of all samples measured by the Archimedes method is also included in Table 1. All values are above 90% of the theoretical value for CCTO and are similar to results reported for doped CCTO [12,27–29].

3.2. Scanning electron microscopy results

The microstructure of all sintered ceramics was investigated by FESEM as shown in Fig. 2. The grain size distribution is shown as insert plots in each SEM micrograph, from which the average grain size was obtained as given in the respective histograms. In general, the grain size

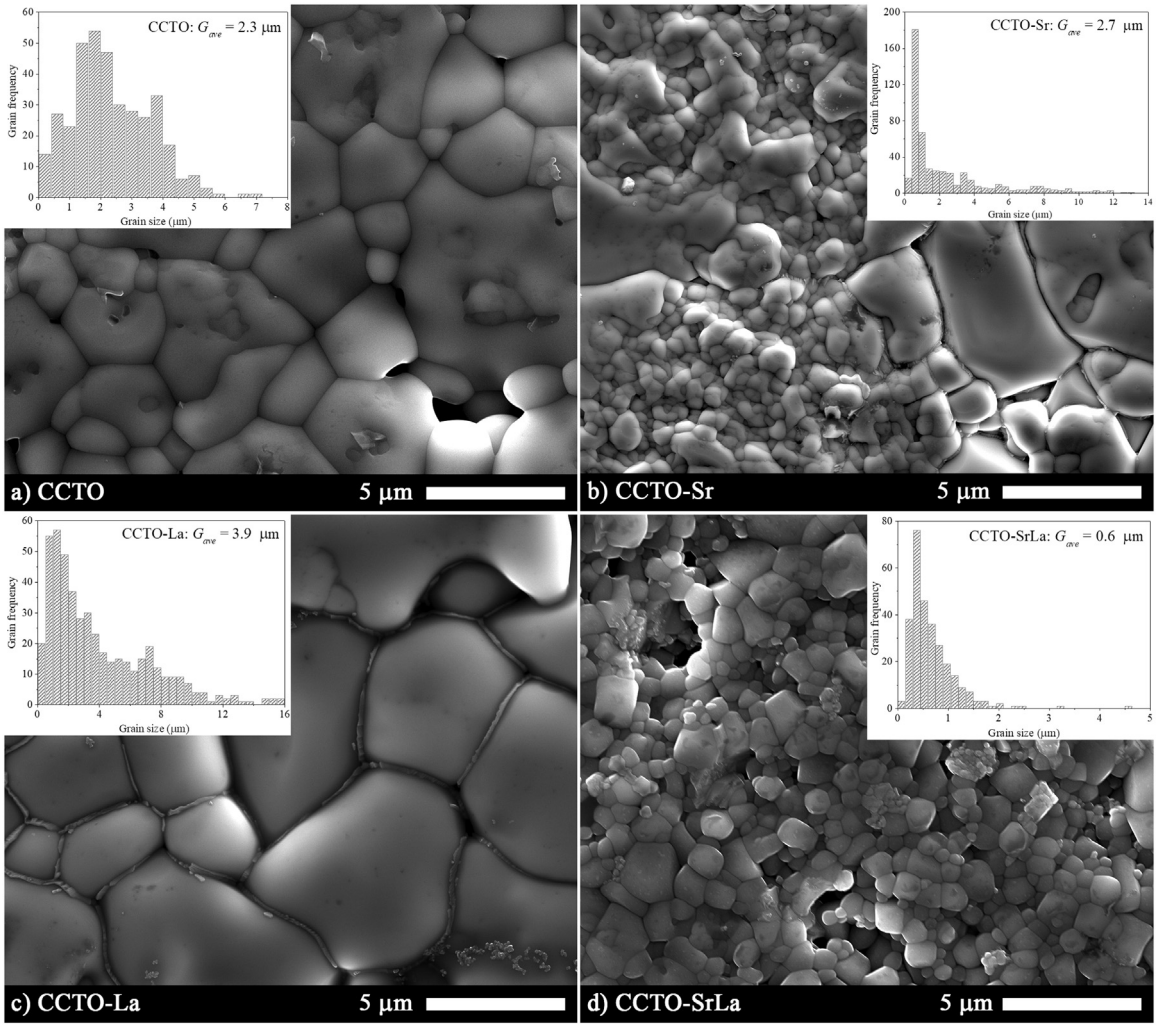

Fig. 2. SEM micrographs of pure and doped CCTO: a) Pure CCTO, b) CCTO-Sr, c) CCTO-La, d) CCTO-SrLa. Insert plots: Grain size distribution for each sample.

Table 2
Elemental quantification from EDX analysis.

Sample	EDX composition (at.-%)					
	Ca	Cu	Ti	O	Sr	La
CCTO	6.1	15.2	20.6	58.1	-	-
CCTO-Sr	4.0	15.2	21.1	58.2	1.6	–
CCTO-La	4.5	16.6	20.0	58.1	–	0.9
CCTO-SrLa	2.7	11.9	16.1	67.2	1.4	0.8

of the samples prepared by reactive sintering are smaller than those of CCTO ceramics prepared by the conventional solid-state methods with a calcination step [15,18,23,30,31]. Pure CCTO sample (Fig. 2(a)) exhibited an abnormal grain growth with an average size of 2.3 μm. Samples CCTO-Sr and CCTO-La (Fig. 2(b) and (c), respectively) also showed an abnormal grain growth that led to a small increase of the average grain size, thus generating a bimodal distribution. These samples also exhibited copper segregation in intergranular regions as detected by EDX. Fig. S2 shows the EDX spectrum of an intergranular region of the CCTO-La sample, which exhibits a higher content of copper compared to the bulk sample given in Fig. S3. The Cu segregation can be related to the thermal etching of the surfaces prior to SEM observations due to the superficial characteristics of the intergranular features, as reported by Felix et al. [32] for similar thermal etching conditions.

For the co-doped CCTO-SrLa sample (Fig. 2d), the average grain size is remarkably reduced by almost 4 times and the abnormal grain growth is also observed. This indicates that the grain growth is inhibited as a result of the simultaneous doping by Sr and La, where the simultaneous substitution of both dopants can balance the driving and restorative forces for grain boundary (GB) migration, as proposed by Boonlakhorn et al. [30]. Similar effects of co-doping in CCTO on the grain size has been reported by Thomas et al. [33] in CCTO co-doped with La/Nb, Ardakani et al. [23] in CCTO doped with Cr/La and Du et al. [27] in the ceramic CCTO-Y/Al.

The microanalysis by EDX of the different samples revealed good dispersion of the major elements (i.e., Ca, Cu, Ti, and O) and of the Sr and La dopants in the single and co–doped ceramics. Quantitative results are summarized in Table 2. The results of the quantification from the different analysis is shown in Table 2, which values were obtained from the EDX spectra exhibited in Supplementary material. No segregation of copper or dopants was observed in the CCTO-SrLa sample.

3.3. Dielectric behavior

Fig. 3(a) presents the frequency dependence of the real permittivity (ε′) at room temperature of the pure and doped CCTO ceramics. Pure CCTO exhibits a plateau at the frequency ranging from 20 Hz to 20 kHz, followed by a rapid decrease in the high frequency range, which can be explained by a Debye-like dipolar relaxation process [15,24,34]. A similar behavior is observed for CCTO-La sample, but with a permittivity one order of magnitude smaller than pure CCTO. The CCTO-Sr sample shows a steep-like behavior in the whole frequency range with a strong decrease around 100 Hz that keeps falling until the MHz region. The co-doped CCTO-SrLa ceramic exhibits similar behavior than the CCTO-La sample but with higher ε′ and a plateau that extends approximately to 1 MHz.

The dielectric loss, or dissipation factor, (tan(δ)) of pure and doped CCTO ceramics shows a strong dependency related to the frequency as shown in Fig. 3(b). Pure CCTO has a minimum tan(δ) of 0.061 at 383 Hz, while, for CCTO-La, lower values can be found at higher frequencies. CCTO-La has a minimum tan(δ) of 0.054 between 10 and 30 kHz, while CCTO-Sr has higher tan(δ) with values over 0.35 in the whole frequency range. In contrast, the co-doped sample has the smallest tan(δ) of 0.039, which is shifted to a higher frequency of 26.8 kHz. Similar results for the dielectric loss have been reported for co-doped CCTO ceramics of different sites in the crystalline structure. For example, Xu et al. [22] and Boonlakhorn et al. [19] reported a value of 0.039 in CCTO co-doped with Y/Zr, and with Sm/Mg, respectively. Ardakani et al. [23] reached a dielectric loss of 0.137 for CCTO co-doped with Cr/La.

Impedance measurements between 55 and 445 K at 10 kHz show that ε′ tends to increase with increasing temperature for all samples, as depicted in Fig. 4(a). CCTO-Sr sample shows significant changes as temperature increases whereas CCTO-La sample demonstrates a high thermal stability above 130 K. Compared to other ceramics, it is remarkable that the CCTO-SrLa sample has the highest thermal stability indicated by a high and almost constant ε′ above 100 K that remains almost constant until high temperature. These results are similar to those observed in the literature [14,19,20,22,23].

Fig. 4(b) shows the evolution of tan(δ) with temperature. It can be seen the relaxation peaks of CCTO-La and CCTO-SrLa samples at lower temperature than CCTO. Pure CCTO sample has higher tan(δ) than doped samples between 75 and 235 K while co-doped sample exhibits the lowest tan(δ) of all samples between 200 and 300 K. Over this last temperature, the CCTO-La sample has the least dissipation loss.

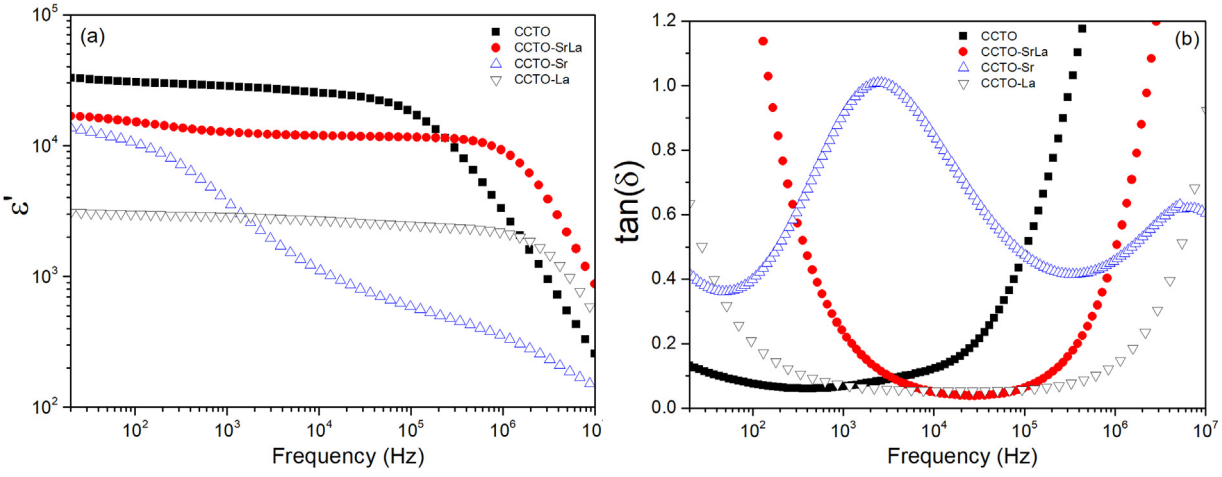

Fig. 3. Frequency dependence of permittivity (a) and dielectric loss (b) of pure and doped samples measured at room temperature.

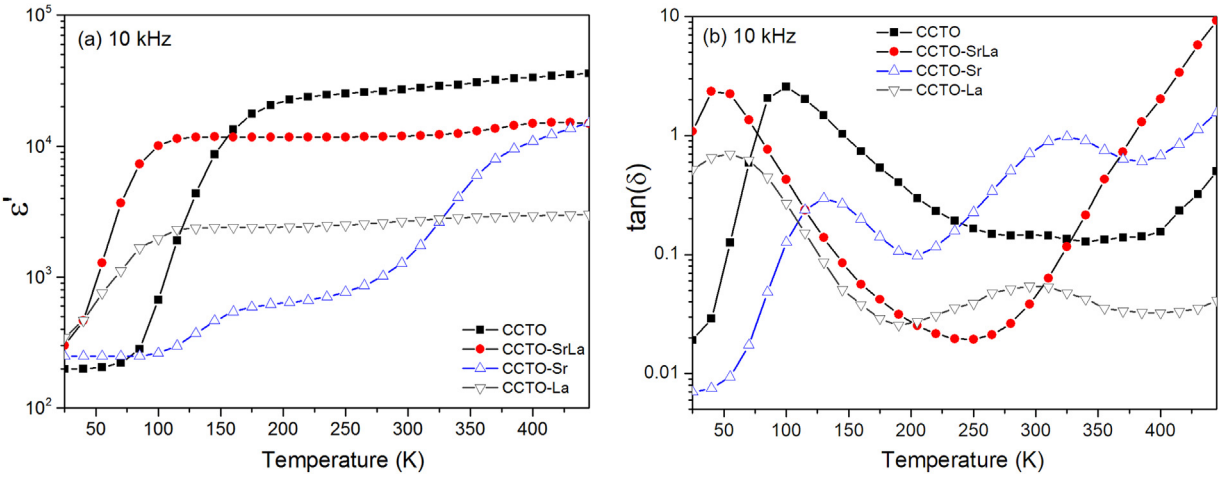

Fig. 4. Temperature dependence of dielectric permittivity and dielectric loss measured at 10 kHz for pure and doped ceramic samples.

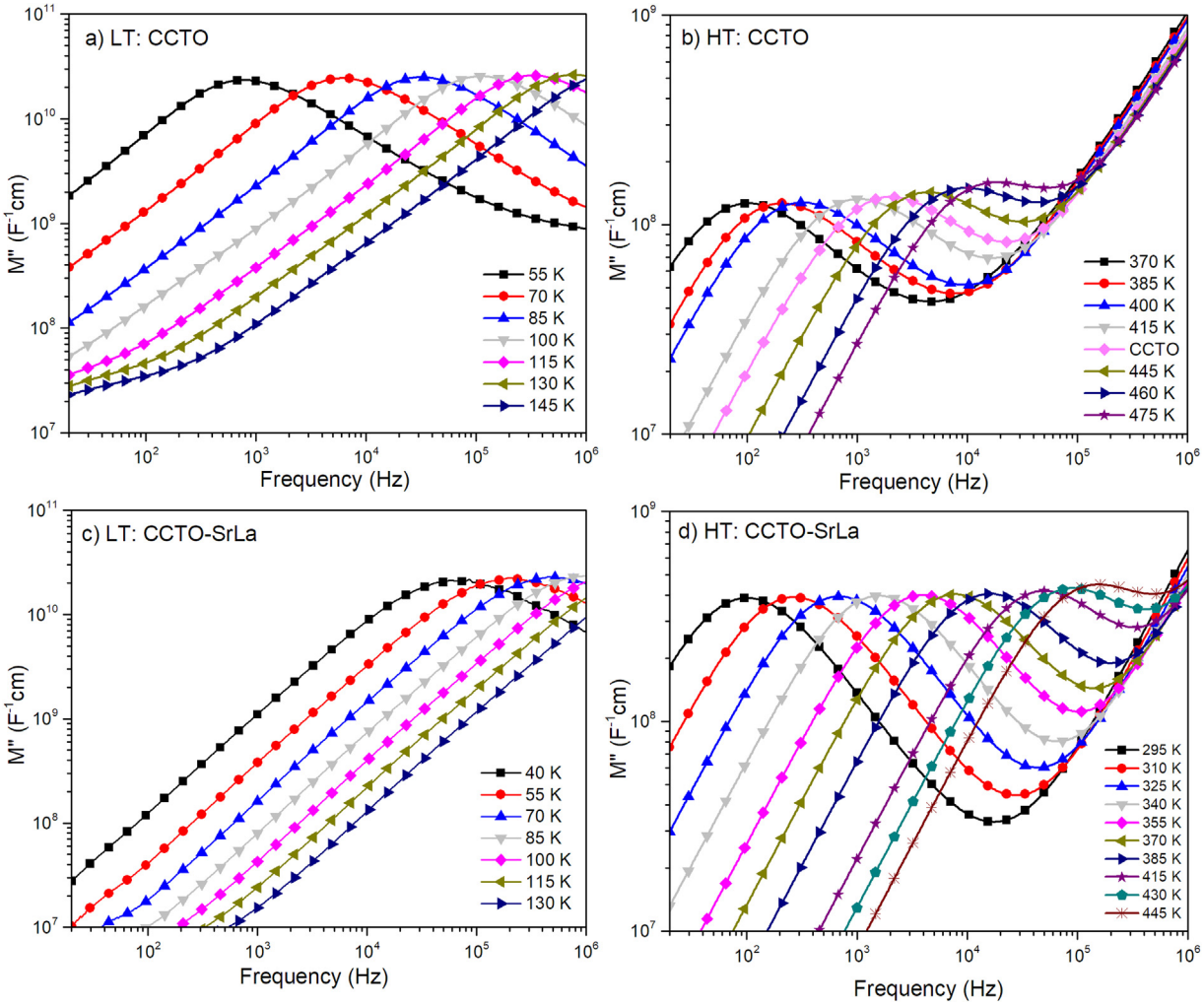

Fig. 5. M″ spectroscopy plots of pure CCTO at low temperatures (a), high temperatures (b); and CCTO-SrLa at low temperatures (c) and high temperatures (d).

3.4. Complex impedance analysis

The electrical modulus is considered to be more effective for analyzing the defect relaxation of polycrystalline ceramics, and is a powerful method to exhibit the resistive and semiconducting components in electrically heterogeneous ceramics such as CCTO [35]. The complex modulus M^* is defined as $1/\varepsilon^*$, where ε^* corresponds to the complex permittivity [36],

$$M^*=M' + iM'' = 1/(\varepsilon' - i\varepsilon'') = \varepsilon'/(\varepsilon'^2+\varepsilon''^2) + i\varepsilon''/(\varepsilon'^2+\varepsilon''^2) \quad (1)$$

where M′ and M″ are the real and imaginary part of complex modulus. Fig. 5 shows the imaginary part versus frequency at different temperatures for CCTO and CCTO-SrLa. In the low temperature range (Fig. 5(a)) CCTO have a pronounced peak that shifts to higher

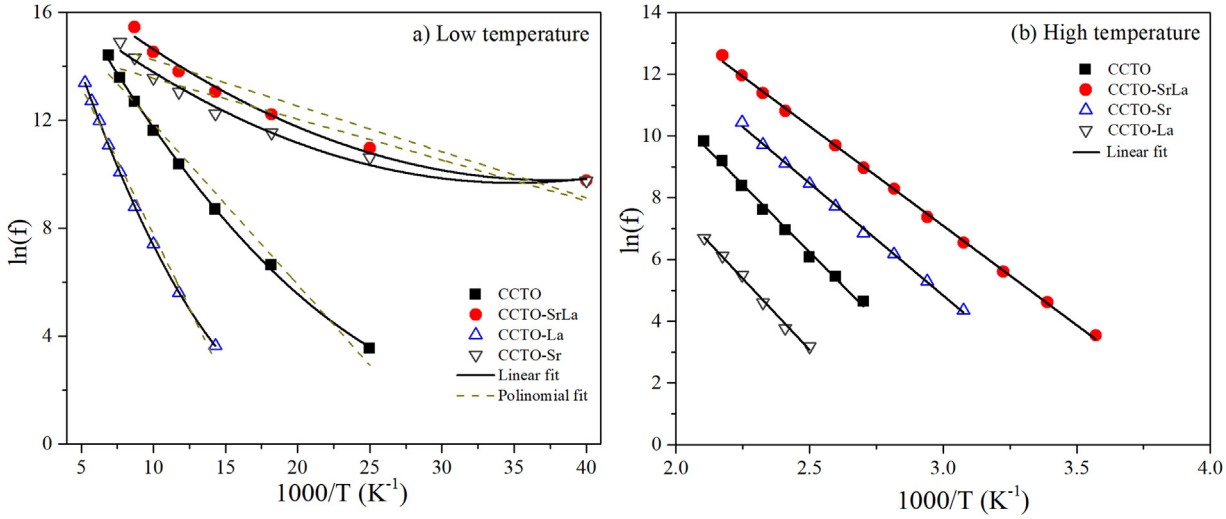

Fig. 6. Natural logarithm of relaxation peak frequency as a function of temperature at (a) low temperature and (b) high temperature.

Table 3
Calculated resistance and activation energy values from low and high temperature measurements.

Sample	Low temperature			High temperature	
	E_a' (meV)	E_a'' (meV)	R_b, 85 K (kΩ cm)	Ea (meV)	R_{gb}, 430 K (kΩ cm)
CCTO	92	10	250	752	21
CCTO-Sr	168	18	8892	627	9
CCTO-La	40	7	12	796	1598
CCTO-SrLa	41	7	6	555	2

frequencies as temperature increases. The measurements in the high temperature range plotted in Fig. 5(b) show that above a temperature of 370 K, a second peak with a lower intensity appears (please refer to the scale) that also shifts to higher frequency with increasing temperature. Single and co-doped ceramics present a similar behavior compared to pure CCTO, as demonstrated in Fig. 5(c) and (d) for CCTO-SrLa. This sample exhibits peaks of comparable intensity but shifted to higher frequencies than pure CCTO at low temperature (Fig. 5(c)). Whereas, at high temperatures, the peaks of CCTO-SrLa where of higher intensity than the undoped sample (Fig. 5(d)).

The shift of these relaxation peaks as a function of the temperature indicates that both electrical responses are thermally activated. Thus, an Arrhenius expression can be used to describe this process:

$$f_P = f_0 \exp(-E_a/k_B T) \quad (2)$$

where f_P is the peak frequency, f_0 is the pre-exponential factor, E_a is the activation energy, and k_B is the Boltzmann constant. The plots of ln(f_P) vs 1/T are depicted in Fig. 6 for measurements at low and high temperatures. It can be seen that the relaxation frequencies at low temperature (Fig. 6(a)) do not follow the Arrhenius Law (red dashed line). However, the data can be well fitted with a polynomial approach as proposed by Chen et al. [37]:

$$f_P = f_0 exp\left[-\frac{E_a'}{k_B T} + \left(\frac{E_a''}{k_B T}\right)^2\right] \quad (3)$$

where E_a' and E_a'' are interaction energies. Chen et al. assigned E_a' to the potential barrier height of the interaction between Ti ions and its six nearest-neighbor O ions, while E_a'' is the correlation among near-neighboring ions. As shown in Fig. 6(a), this polynomial relation fits the data well, especially for samples that showed relaxation at lower temperatures, which indicates a correlation with the hopping of Ti ions or defects [37]. The values of both calculated energies are listed in Table 2 for all samples.

It is clear that for all samples E_a' is higher than E_a'' with typical ranges between 40 and 168 meV. These values of activation energies have been generally considered to be intrinsic bulk or grain activation energy of CCTO ceramics [3,9,19,35–37]. For pure CCTO, this value is close to 100 meV, which is in good agreement with the values obtained

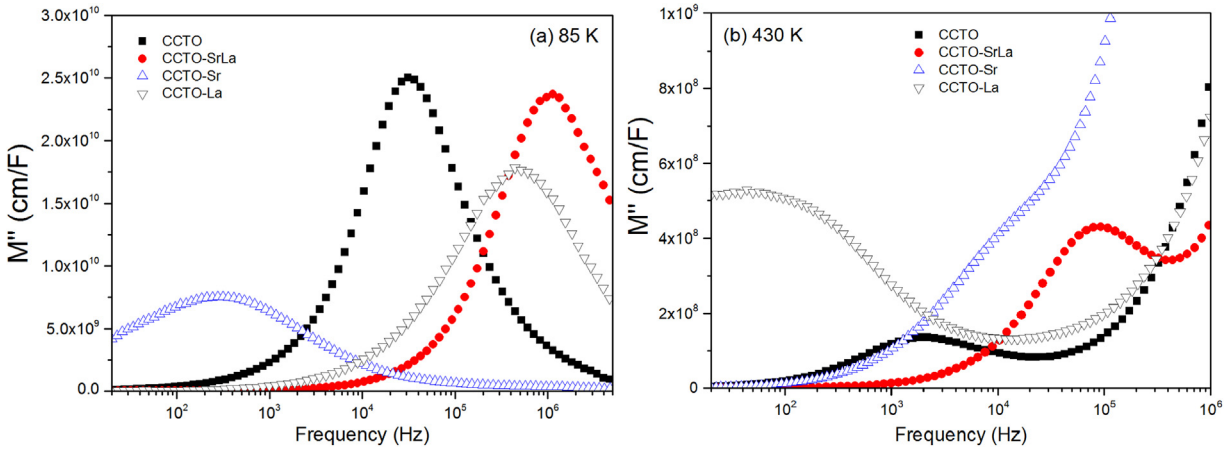

Fig. 7. M″ spectroscopy plots of all ceramics under study at (a) 85 K and (b) 430 K.

for the undoped sample in this study. Moreover, a smaller value of E_a'' is associated with a lower correlation between near-neighboring ions and therefore a higher dissipation factor, which possibly explains the tan(δ) peak at lower temperature of doped CCTO-La and CCTO-SrLa (Fig. 4(b)).

In contrast, the relaxation peaks at high temperature do follow an Arrhenius law as shown in Fig. 6(b), from which the activation energies, E_a, given in Table 3 can be calculated. The values range between 555 and 796 meV. These values are related to domain or grain boundaries according to the literature [3,9,19,35–37]. The lower value of the activation energy for the CCTO-SrLa may be a the result of a higher density of oxygen vacancies and free electrons at the grain boundaries [33], produced by the simultaneous doping of Sr and La.

In summary, from the activation energies and according to the modulus′ analysis, the bulk response is manifested under cryogenic conditions as a large M″ Debye peak, while the grain boundary response is revealed above room temperature.

The different activation energy behavior of the bulk and the grain boundaries can be associated to an internal barrier layer capacitor (IBLC) structure [13,35,38], consisting of semi-conducting grains separated by thin insulating grain boundaries (GBs) leading to high ε′ values observed in CCTO. Using the M″ peaks observed at different temperatures, it is possible to directly calculate the resistance of the bulk grains, R_b, and the grain boundaries, R_{gb}, using the following relations at low and high temperatures [35], respectively:

$$M''(f_{max}) \approx \frac{C_0}{2C} \tag{4}$$

$$R = \frac{1}{2\pi C f_{max}} \tag{5}$$

where C_0 represents the capacitance of the empty cell in vacuum. Fig. 7(a) depicts a comparative plot of M″ measured at 85 K of all samples. It is clear that all samples have a M''_{max} peak at distinctive frequencies and that the maximum intensities can be found for CCTO and CCTO-SrLa. From these peaks and using Eqs. (4) and (5), the values for R_b (Table 3) can be calculated. In this context, CCTO-SrLa exhibits the lowest bulk grain resistance while CCTO-Sr has the highest R_b. The behavior of ε′ at 85 K of different samples (Fig. 4(a)) shows that there is a relation between R_b and the dielectric permittivity: the highest ε′ is of CCTO-SrLa sample (lowest R_b) while the lowest ε′ is for CCTO-Sr (highest R_b).

Similarly, M″ plots of the impedance measurements at 430 K are depicted in Fig. 7(b). The smallest peak corresponds to CCTO. The calculated R_{gb} values from M″ peaks are also included in Table 3. In this case, CCTO-La has a grain boundary resistance 3 order of magnitude higher than the other samples. In contrast, CCTO-SrLa has the smallest value. At 430 K, the influence of R_{gb} is observed in the tan(δ) plot of Fig. 4(b), where the lowest loss is for CCTO-La sample (highest R_{gb}) and the contrary is for CCTO-SrLa ceramic (lowest R_{gb}).

From the IBLC model [3,11,15,24], the frequency dependence of tan (δ) can be explained using the equation:

$$tan(\delta) = \frac{1}{\omega R_{gb} C_P} + \omega R_b C_P \tag{6}$$

where ω is the angular frequency and C_P is the effective capacitance of the system. The value of tan(δ) in the low frequency range is usually due to the dc conductivity, which is governed by R_{gb}. Thus, Eq. (6) qualitatively agrees with the results shown in Fig. 3(b), where in the low frequency range, lower tan(δ) values were obtained for samples with higher R_{gb} (single doped sample CCTO-La). At higher frequencies, the dielectric loss behavior is dominated by the bulk response, which in our case corresponds to the sample CCTO-SrLa showing the lowest R_b.

Based upon these results, it can be concluded that the optimal dielectric property can be achieved by co-doping. The simultaneous doping by Sr and La of CCTO allows to obtain a ceramic with lower dielectric loss without a strong degradation of the dielectric constant over a wide range of temperatures.

4. Conclusions

The dielectric properties of CCTO ceramics were successfully improved by co-doping with Sr and La, prepared by mechano-synthesis using mixing and further consolidation by reactive sintering without a calcination step. Co-doped CCTO-SrLa ceramic showed the smallest tan (δ) of 0.039 at 26.8 kHz compared to pure CCTO and single-doped ceramics. The co-doped sample reached a higher dielectric permittivity compared to the single-doped ceramics. It is remarkable that in comparison to other ceramics, CCTO-SrLa has the highest thermal stability indicated by a high and almost constant value for ε′ above 100 K. In addition, the co-doped sample showed the lowest tan(δ) of all samples between 200 and 300 K. This behavior can be attributed to the lower bulk resistance for the co-doped sample.

Acknowledgements

R. Espinoza acknowledges the financial support of the Fondecyt Project 1150652, while S. Hevia would like to thanks to the project Fondequip EQM150101. Both projects from the Chilean National Commission for Scientific and Technological Research, CONICYT.

Appendix A. Supporting information

Supplementary data associated with this article can be found in the online version at http://dx.doi.org/10.1016/j.ceramint.2018.05.223.

References

[1] S. Krohns, P. Lunkenheimer, S. Meissner, A. Reller, B. Gleich, A. Rathgeber, T. Gaugler, H.U. Buhl, D.C. Sinclair, A. Loidl, The route to resource-efficient novel materials, Nat. Mater. 10 (2011) 899–901, http://dx.doi.org/10.1038/nmat3180.
[2] J. Lee, J. Koh, Grain size effects on the dielectric properties of $CaCu_3Ti_4O_{12}$ ceramics for supercapacitor applications, Ceram. Int. 41 (2015) 10442–10447, http://dx.doi.org/10.1016/j.ceramint.2015.04.109.
[3] P. Kumar, K.L. Yadav, Dwell time effect on the barrier layer capacitor structure, Ceram. Int. 41 (2015) 12386–12392, http://dx.doi.org/10.1016/j.ceramint.2015.06.072.
[4] S.Y. Chung, I.D. Kim, S.J. Kang, Strong nonlinear current-voltage behaviour in perovskite-derivative calcium copper titanate, Nat. Mater. 3 (2004) 774–778, http://dx.doi.org/10.1038/nmat1238.
[5] L. He, J. Neaton, D. Vanderbilt, M. Cohen, Lattice dielectric response of $CdCu_3Ti_4O_{12}$ and $CaCu_3Ti_4O_{12}$ from first principles, Phys. Rev. B 67 (2003), http://dx.doi.org/10.1103/PhysRevB.67.012103.
[6] D.C. Sinclair, T.B. Adams, F.D. Morrison, A.R. West, D.C. Sinclair, T.B. Adams, F.D. Morrison, A.R. West, $CaCu_3Ti_4O_{12}$: one-step internal barrier layer capacitor, Appl. Phys. Lett. 2153 (2012) 67–70, http://dx.doi.org/10.1063/1.1463211.
[7] A.P. Ramirez, M.A. Subramanian, M. Gardela, G. Blumberga, D. Li, T. Vogt, S.M. Shapiro, Giant dielectric constant response in a copper-titanate, Solid State Commun. 115 (2000) 217–220, http://dx.doi.org/10.1016/S0038-1098(00)00182-4.
[8] P. Lunkenheimer, R. Fichtl, S. Ebbinghaus, A. Loidl, Nonintrinsic origin of the colossal dielectric constants in CaCu3Ti4O12, Phys. Rev. B 70 (2004), http://dx.doi.org/10.1103/PhysRevB.70.172102.
[9] M. Li, A. Feteira, D.C. Sinclair, A.R. West, Influence of Mn doping on the semiconducting properties of $CaCu_3Ti_4O_{12}$ ceramics, Appl. Phys. Lett. 88 (2006) 232903, http://dx.doi.org/10.1063/1.2200732.
[10] S.-Y. Chung, S.-Y. Choi, T. Yamamoto, Y. Ikuhara, S.-J.L. Kang, Site-selectivity of 3d metal cation dopants and dielectric response in calcium copper titanate, Appl. Phys. Lett. 88 (2006) 91917, http://dx.doi.org/10.1063/1.2179110.
[11] L. Feng, X. Tang, Y. Yan, X. Chen, Z. Jiao, G. Cao, Decrease of dielectric loss in $CaCu_3Ti_4O_{12}$ ceramics by La doping, Phys. Status Solidi 203 (2006) R22–R24, http://dx.doi.org/10.1002/pssa.200622038.
[12] S. Jin, H. Xia, Y. Zhang, Effect of La-doping on the properties of $CaCu_3Ti_4O_{12}$ dielectric ceramics, Ceram. Int. 35 (2009) 309–313, http://dx.doi.org/10.1016/j.ceramint.2007.10.007.
[13] C. Mu, H. Zhang, Y. Liu, Y. Song, P. Liu, Rare earth doped $CaCu_3Ti_4O_{12}$ electronic ceramics for high frequency applications, J. Rare Earths 28 (2010) 43–47, http://dx.doi.org/10.1016/s1002-0721(09)60048-x.
[14] H. Xue, X. Guan, R. Yu, Z. Xiong, Dielectric properties and current–voltage nonlinear behavior of $Ca_{1-x}Sr_xCu_3Ti_4O_{12}$ ceramics, J. Alloy. Compd. 482 (2009) L14–L17, http://dx.doi.org/10.1016/j.jallcom.2009.03.190.
[15] J.L. Zupei Yang, Lijuan Zhang, Xiaolian Chao, Lirong Xiong, High permittivity and

low dielectric loss of the $Ca_{1-x}Sr_xCu_3Ti_4O_{12}$ ceramics, J. Alloy. Compd. 509 (2011) 8716–8719, http://dx.doi.org/10.1016/j.jallcom.2011.06.039.
[16] S. Vangchangyia, T. Yamwong, E. Swatsitang, P. Thongbai, S. Maensiri, Selectivity of doping ions to effectively improve dielectric and non-ohmic properties of $CaCu_3Ti_4O_{12}$ ceramics, Ceram. Int. 39 (2013) 8133–8139, http://dx.doi.org/10.1016/j.ceramint.2013.03.086.
[17] A.K. Rai, N.K. Singh, S.K. Acharya, L. Singh, K.D. Mandal, Effect of tantalum substitutions on microstructures and dielectric properties of calcium copper titanate ($CaCu_3Ti_4O_{12}$) ceramic, Mater. Sci. Eng. B 177 (2012) 1213–1218, http://dx.doi.org/10.1016/j.mseb.2012.06.002.
[18] R. Xue, G. Zhao, J. Chen, Z. Chen, D. Liu, Effect of doping ions on the structural defect and the electrical behavior of $CaCu_3Ti_4O_{12}$ ceramics, Mater. Res. Bull. 76 (2016) 124–132, http://dx.doi.org/10.1016/j.materresbull.2015.12.020.
[19] J. Boonlakhorn, P. Kidkhunthod, P. Thongbai, A novel approach to achieve high dielectric permittivity and low loss tangent in $CaCu_3Ti_4O_{12}$ ceramics by co-doping with Sm3+ and Mg2+ ions, J. Eur. Ceram. Soc. 35 (2015) 3521–3528, http://dx.doi.org/10.1016/j.jeurceramsoc.2015.06.008.
[20] J. Boonlakhorn, B. Putasaeng, P. Kidkhunthod, P. Thongbai, Improved dielectric properties of (Y + Mg) co-doped $CaCu_3Ti_4O_{12}$ ceramics by controlling geometric and intrinsic properties of grain boundaries, Mater. Des. 92 (2016) 494–498, http://dx.doi.org/10.1016/j.matdes.2015.12.042.
[21] À. Ca, À. Cu, O. Ti, J. Boonlakhorn, P. Kidkhunthod, P. Thongbai, S. Maensiri, Colossal dielectric permittivity and electrical properties of the grain boundary of $Ca_{1-3x/2}Yb_xCu_{3-y}Mg_yTi_4O_{12}$ (x = 0.05, y = 0.05 and 0.30), Ceram. Int. 42 (2016) 8467–8472, http://dx.doi.org/10.1016/j.ceramint.2016.02.067.
[22] Z. Xu, H. Qiang, Y. Chen, Z. Chen, Microstructure and enhanced dielectric properties of yttrium and zirconium co-doped $CaCu_3Ti_4O_{12}$ ceramics, Mater. Chem. Phys. 191 (2017) 1–5, http://dx.doi.org/10.1016/j.matchemphys.2017.01.015.
[23] H.A. Ardakani, M. Alizadeh, R. Amini, M.R. Ghazanfari, Dielectric properties of $CaCu_3Ti_4O_{12}$ improved by chromium/lanthanum co-doping, Ceram. Int. 38 (2012) 4217–4220, http://dx.doi.org/10.1016/j.ceramint.2012.02.005.
[24] A.K. Thomas, K. Abraham, J. Thomas, K.V. Saban, Structural and dielectric properties of A- and B-sites doped $CaCu_3Ti_4O_{12}$ ceramics, Ceram. Int. 41 (2015) 10250–10255, http://dx.doi.org/10.1016/j.ceramint.2015.04.138.
[25] M.A. de la Rubia, P. Leret, A. del Campo, R.E. Alonso, A.R. López-Garcia, J.F. Fernández, J. de Frutos, Dielectric behaviour of Hf-doped $CaCu_3Ti_4O_{12}$ ceramics obtained by conventional synthesis and reactive sintering, J. Eur. Ceram. Soc. 32 (2012) 1691–1699, http://dx.doi.org/10.1016/j.jeurceramsoc.2012.01.024.
[26] R. Espinoza-González, E. Vega, R. Tamayo, J.M. Criado, M.J. Diánez, Mechanochemical processing of $CaCu_3Ti_4O_{12}$ with giant dielectric properties, Mater. Manuf. Process. (2014), http://dx.doi.org/10.1080/10426914.2014.921702 (140516112214009).
[27] G. Du, F. Wei, W. Li, N. Chen, Co-doping effects of A-site Y3+ and B-site Al3+ on the microstructures and dielectric properties of $CaCu_3Ti_4O_{12}$ ceramics, J. Eur. Ceram. Soc. 37 (2017) 4653–4659, http://dx.doi.org/10.1016/j.jeurceramsoc.2017.06.046.
[28] J. Boonlakhorn, P. Kidkhunthod, P. Thongbai, A novel approach to achieve high dielectric permittivity and low loss tangent in $CaCu_3Ti_4O_{12}$ ceramics by co-doping with Sm^{3+} and Mg^{2+} ions, J. Eur. Ceram. Soc. 35 (2015) 3521–3528, http://dx.doi.org/10.1016/j.jeurceramsoc.2015.06.008.
[29] Z. Tang, Y. Huang, K. Wu, J. Li, Significantly enhanced breakdown field in $Ca_{1-x}Sr_xCu_3Ti_4O_{12}$ ceramics by tailoring donor densities, J. Eur. Ceram. Soc. 38 (2018) 1569–1575, http://dx.doi.org/10.1016/j.jeurceramsoc.2017.11.018.
[30] J. Boonlakhorn, P. Kidkhunthod, N. Chanlek, P. Thongbai, (Al^{3+}, Nb^{5+}) co–doped $CaCu_3Ti_4O_{12}$: an extended approach for acceptor–donor heteroatomic substitutions to achieve high–performance giant–dielectric permittivity, J. Eur. Ceram. Soc. 38 (2018) 137–143, http://dx.doi.org/10.1016/j.jeurceramsoc.2017.08.040.
[31] J. Boonlakhorn, P. Thongbai, Enhanced non-Ohmic properties and giant dielectric response of (Sm+Zn) co-doped $CaCu_3Ti_4O_{12}$ ceramics, Ceram. Int. 43 (2017) 12736–12741, http://dx.doi.org/10.1016/j.ceramint.2017.06.159.
[32] A.A. Felix, V.D.N. Bezzon, M.O. Orlandi, D. Vengust, M. Spreitzer, E. Longo, D. Suvorov, J.A. Varela, Role of oxygen on the phase stability and microstructure evolution of $CaCu_3Ti_4O_{12}$ ceramics, J. Eur. Ceram. Soc. 37 (2017) 129–136, http://dx.doi.org/10.1016/j.jeurceramsoc.2016.07.039.
[33] A.K. Thomas, K. Abraham, J. Thomas, K.V. Saban, Structural and dielectric properties of A- and B-sites doped $CaCu_3Ti_4O_{12}$ ceramics, Ceram. Int. 41 (2015) 10250–10255, http://dx.doi.org/10.1016/j.ceramint.2015.04.138.
[34] T. Li, H.F. He, T. Zhang, B. Zhao, Z.Q. Chen, H.Y. Dai, R.Z. Xue, Z.P. Chen, Effect of synthesizing temperatures on the microstructure and electrical property of $CaCu_3Ti_4O_{12}$ ceramics prepared by sol-gel process, J. Alloy. Compd. 684 (2016) 315–321, http://dx.doi.org/10.1016/j.jallcom.2016.05.177.
[35] S.I.R. Costa, M. Li, J.R. Frade, D.C. Sinclair, Modulus spectroscopy of $CaCu_3Ti_4O_{12}$ ceramics: clues to the internal barrier layer capacitance mechanism, RSC Adv. 3 (2013) 7030–7036, http://dx.doi.org/10.1039/C3RA40216A.
[36] J. Li, X. Zhao, F. Gu, S. Li, Defects and dc electrical degradation in $CaCu_3Ti_4O_{12}$ ceramics: role of oxygen vacancy migration, Appl. Phys. Lett. 100 (2012) 202905, http://dx.doi.org/10.1063/1.4720151.
[37] K. Chen, Y. Liu, F. Gao, Z. Du, J. Liu, X. Ying, X. Lu, J. Zhu, Ti deficiency effect on the dielectric response of $CaCu_3Ti_4O_{12}$ ceramics, Solid State Commun. 141 (2007) 440–444, http://dx.doi.org/10.1016/j.ssc.2006.12.004.
[38] R. Schmidt, M.C. Stennett, N.C. Hyatt, J. Pokorny, J. Prado-Gonjal, M. Li, D.C. Sinclair, Effects of sintering temperature on the internal barrier layer capacitor (IBLC) structure in $CaCu_3Ti_4O_{12}$ (CCTO) ceramics, J. Eur. Ceram. Soc. 32 (2012) 3313–3323, http://dx.doi.org/10.1016/j.jeurceramsoc.2012.03.040.